EUROPEAN ORGANIZATION FOR NUCLEAR RESEARCH

CERN–EP/99-31
February 19, 1999

The Polarized Double Cell Target of the SMC

The Spin Muon Collaboration (SMC)

Abstract

The polarized target of the Spin Muon Collaboration at CERN was used for deep inelastic muon scattering experiments during 1993 to 1996 with a polarized muon beam to investigate the spin structure of the nucleon. Most of the experiments were carried out with longitudinal target polarization and 190 GeV muons, and some were done with transverse polarization and 100 GeV muons. Protons as well as deuterons were polarized by dynamic nuclear polarization (DNP) in three kinds of solid materials – butanol, ammonia, and deuterated butanol, with maximum degrees of polarization of 94, 91, and 60 %, respectively. Considerable attention was paid to the accuracies of the NMR polarization measurements and their analyses. The achieved accuracies were between 2.0 and 3.2 %. The SMC target system with two cells of opposite polarizations, each cell 65 cm long and 5 cm in diameter, constitutes the largest polarized target system ever built and facilitates accurate spin asymmetry measurements. The design considerations, the construction and its performance over the years are reviewed.

To be submitted to NIM A

1 Introduction

An extensive programme to study the spin dependent structure functions of the nucleon has been carried out at CERN by the Spin Muon Collaboration (SMC). In the past few years results from the SMC measurements [1, 2, 3, 4, 5, 6, 7, 8], those from SLAC [9, 10, 11, 12, 13, 14, 15, 16], and recently from HERMES [17] have improved the knowledge on the internal spin structure of the proton and neutron considerably.

In the SMC experiments, we made use of deep inelastic scattering (DIS) of longitudinally polarized muons off polarized protons and deuterons to study the internal spin structure of the nucleons. Since the secondary muon beam from the CERN SPS had a low flux ($4 \cdot 10^7$ μ/pulse, pulse interval 14.4 s), and since the muon cross section for scattering is small, a large polarized target with high spin density was essential to our measurements. The data taking by the SMC started in 1991 with the polarized target used by the European Muon Collaboration [18] and modified by the SMC for the first measurements with polarized deuterons [19].

Later data taking was carried out with a completely new polarized double cell target system. A short overview of this SMC target has been published [20]. Here we give a comprehensive report on the design of the SMC polarized target and on the experience gained from its operation during 1993 to 1996, notably on the way the target polarization was measured and evaluated.

After a brief overview in section 2 of the method used to obtain the spin dependent structure functions, we describe in section 3 the design, construction and operation of the target system, and in section 4 the polarization measurements and analyses. In section 5 relaxation data and transverse polarization are briefly discussed. In section 6 we summarize our main results and achievements related to the SMC polarized target.

2 Basics of spin asymmetry measurements

The measurement of the spin dependent structure functions $g_1^{p,d}$ of the proton and the deuteron enables the study of the internal spin structure of the nucleon. Theoretical predictions for the spin sum rules exist and can be tested using the results of polarized deep inelastic scattering experiments. In most of our measurements we determined the longitudinal spin asymmetry $A_\parallel^{p,d} = (\sigma^{\uparrow\downarrow} - \sigma^{\uparrow\uparrow})/(\sigma^{\uparrow\downarrow} + \sigma^{\uparrow\uparrow})$ for muon-nucleon scattering with antiparallel and parallel spins along the muon beam direction, both for polarized protons and deuterons. In some of our experiments, about 5% of the data taking, the transverse spin asymmetry $A_\perp^{p,d}$, corresponding to transverse nucleon spin orientations with respect to the scattering plane, were measured. These asymmetries are related to the proton and deuteron virtual photon asymmetries $A_1^{p,d}$ and $A_2^{p,d}$ according to

$$A_\parallel^{p,d} = D(A_1^{p,d} + \eta A_2^{p,d}), \qquad A_\perp^{p,d} = d(A_2^{p,d} - \xi A_1^{p,d}), \tag{1}$$

in which the factors η and ξ depend only on kinematic variables and are small in our experiment, the depolarization factors D and d depend on kinematical variables and on the ratio $R = \sigma_L/\sigma_T$ of longitudinal and transverse photo-absorption cross sections.

Because of the small influence of $A_2^{p,d}$ in our longitudinal polarization experiments, the longitudinal asymmetry $A_\parallel^{p,d}$ can directly be related to the spin structure function $g_1^{p,d}$ by

$$g_1^{p,d}(x, Q^2) \approx \frac{F_2(x, Q^2)}{2x(1 + R(x, Q^2))} \frac{A_\parallel^{p,d}}{D} , \tag{2}$$

where $F_2(x, Q^2)$ is the unpolarized structure function, $-Q^2$ is the square of the four-momentum of the virtual photon exchanged between the muon and the nucleon, while $x = Q^2/(2M\nu)$ is the Bjorken scaling variable representing the fraction of momentum carried by the struck parton.

Here M is the nucleon mass and ν is the energy of the virtual photon. For a longitudinally polarized target the measured event yield, N, can be related to the longitudinal spin asymmetry;

$$N = n\Phi a\sigma_0(1 - fP_\mu PA_\parallel) \ , \tag{3}$$

where n is the number of target nucleons, Φ the beam flux, a the apparatus acceptance, σ_0 the unpolarized (i.e. spin averaged) cross section, f the target dilution factor (defined in Eq. (6)), and P_μ, and P the beam and target polarizations, respectively. The asymmetry cannot be reliably extracted from two consecutive measurements with opposite target polarizations because the relative beam flux cannot be controlled with sufficient accuracy. Therefore, we opted for two oppositely polarized target cells in line along the beam, labelled "upstream" and "downstream", so that the two cells were exposed simultaneously to the same beam flux. The two cells of this target were separated by a suitable distance to allow distinction between events coming from each cell.

The remaining problem was that the ratio, $r = n_u a_u / n_d a_d$, concerning the number of nucleons times the apparatus acceptance for upstream and downstream cells, was not precisely known. The solution was to perform two consecutive measurements separated by a reversal of the polarization in both cells. Then, the expression for the asymmetry becomes

$$A_\parallel = \frac{-1}{2fP_\mu P}\left(\frac{N_u - N_d}{N_u + N_d} - \frac{N'_u - N'_d}{N'_u + N'_d}\right), \tag{4}$$

where N_u and N_d (N'_u and N'_d) are the number of DIS events from the upstream and downstream cells before (after) the polarization reversal. In this expression the ratio r cancels except for a variation $\Delta r = r - r'$ resulting in a systematic error

$$\Delta A_\parallel = \frac{1}{4fP_\mu P}\frac{\Delta r}{r} \ . \tag{5}$$

In order to obtain a sufficiently small systematic error the target system had to be designed to allow frequent reversals of spins with little or no loss of target polarization.

For the two kinds of spin asymmetry measurements it was necessary to have a reliable and safe capability to reverse the longitudinal spin directions and to rotate the polarization from longitudinal to transverse. The knowledge of $A_2^{p,d}$ in the expression for the longitudinal spin asymmetry $A_\parallel^{p,d}$ (see Eq. (1)) was needed for a precise determination of $A_1^{p,d}$.

It is important to obtain the highest possible degree of polarization. From a statistical error point of view an increase of the target polarization by a certain factor is equivalent to an increase of the number of events for a given running time by this factor squared (see Eq. (4)). Since the experiment aimed at a precise asymmetry measurement, for which systematic uncertainties were reduced to the order of 10^{-2}, the target polarization had to be known with a similar accuracy.

The polarized target system was designed with these considerations in mind. In what follows we describe how the high degrees of polarization in the target cells were obtained and how these polarizations were measured accurately.

3 Design of the target

A solid polarized target has several important properties, in particular the inherently high and stable nucleon density and the high polarization obtained by using the technique of dynamic nuclear polarization (DNP) [21]. It is possible to obtain proton polarizations close to 100%. The polarization can be measured to a high accuracy.

DNP is obtained at temperatures below about 1 K, using a homogeneous magnetic field to polarize paramagnetic spins to a high degree, and a microwave field to transfer the polarization to the nuclear spins. For the samples used in our experiments DNP is not well described by the so-called "solid-state" effect in which for sufficiently dilute systems the interaction between paramagnetic spins can be neglected [52], but rather by the cooling (by microwave pumping) of the paramagnetic spin-spin interaction "reservoir" [53]. Therefore, by the coupling of the nuclear spin and the paramagnetic spin systems the nuclei become polarized. Nuclear spin relaxation must be orders of magnitude slower than the relaxation of the dilute paramagnetic centres such that the latter can be used repeatedly to flip the nuclear spins into the preferred direction. Spin diffusion is an additional important phenomenon in this process. Depending on the tuning of the microwave frequency the proton or deuteron spins become polarized parallel or antiparallel to the magnetic field.

The low intensity muon beam and the small size of the muon cross section made it necessary to use a thick target. On the basis of the argument given in Sec. 2 we designed a target with two cells in line, each 60 cm (later 65 cm) long separated by 30 cm (later 20 cm). The designed target diameter was 5 cm consistent with the expected beam profile. The long target forced us to look into the design of a superconducting solenoid which could provide a very homogeneous longitudinal field over at least 150 cm. The chosen field strength was 2.5 T which allowed us to use two available microwave sources of about 70 GHz. A saddle type coil was superposed on the solenoid coil to produce a dipole field of 0.5 T perpendicular to the solenoid field and to enable (1) a relatively fast and reliable reversal of the nuclear spins by field rotation about 180°, and (2) to rotate after DNP the polarization in a field of 0.5 T from longitudinal to transverse direction. With the spins in a field of 0.5 T, thus with the microwaves off, it is necessary to have a target temperature well below 0.1 K in order to achieve long relaxation times. Therefore, a dilution refrigerator was designed (1) to absorb a large amount of microwave power of about 1 W during DNP at about 0.5 K, and (2) to cool the large amount of target material rapidly to well below 0.1 K after the microwave power is turned off. Fig. 1 shows the lay-out of the dilution refrigerator and the magnet system of the target.

A nuclear magnetic resonance (NMR) system with 10 coils was designed to determine the polarizations in the two target cells. To achieve accurate and reliable determinations of the degree of polarizations over the complete target volume is not a trivial matter. Therefore, much attention was paid to the design of the NMR coils, cabling to the electronics, the electronic NMR units and the analysis of the acquired NMR signals.

In the following, we discuss the technical realization of the main components of this double cell polarized target system, i.e., the material, the dilution refrigerator, the magnets, the microwave system and the NMR system. A detailed discussion of the systematic uncertainties of the derived polarizations follows for the different target materials.

3.1 Target Materials

In the case of polarized solid-state targets unpaired electron spins with a density in the range of 10^{19} to 10^{20} cm^{-3} are needed for the DNP process to work well. Depending on the material, these can be introduced by chemical doping with a paramagnetic compound or by irradiation which creates free radicals. In the SMC experiment the radiation damage due to the low-intensity muon beam was negligible and did not limit the choice of material. Both methods of introducing unpaired electrons were used. In 1993, butanol (C_4H_9OH) was used as a proton target, in 1994 and in 1995, deuterated butanol (C_4D_9OD) as a target, and in 1996, ammonia (NH_3) again as a proton target.

The dilution factor f is defined in our case as the fraction of events scattered off the

Table 1: The elements and their respective moles contributing to the target.

Element	Material		
	butanol	d-butanol	ammonia
	n_{A} (mole)	n_{A} (mole)	n_{A} (mole)
^{1}H	185.7	1.2	226
^{2}H	–	206.2	–
^{3}He	6.5 ± 1.0	4.7 ± 1.0	5.4 ± 1.0
^{4}He	23.6 ∓ 1.5	26.6 ∓ 1.5	30.7 ∓ 1.5
C	71.8	80.2	0.22
N	–	–	75.4
O	22.7	25.1	–
F	0.24	–	0.45
Na	0.17	0.18	–
Cr	0.17	0.18	–
Ni	0.14	–*)	0.25
Cu	0.36	–*)	0.58

*) In 1994 the NMR coils were not embedded in the material.

polarizable nucleons under study,

$$f = \left(1 + \sum_A \frac{n_A \cdot \sigma_A}{n_{\mathrm{p(d)}} \cdot \sigma_{\mathrm{p(d)}}}\right)^{-1}, \tag{6}$$

where n is the number of nuclei and σ the unpolarized scattering cross-section per nucleus (proton, deuteron or elements with the atomic weight A). Due to different dependences of σ_A and $\sigma_{p,d}$ on the Bjorken-x, the dilution factor varies with x as is shown in Fig. 2 for the three target materials. Apart from the target material, the dilution factors depended on the ^{3}He/^{4}He cooling mixture, whose composition varied with the temperature, and on the embedded NMR coils with their support structure. The amounts of the elements in each cell are given in Table 1.

Butanol is a clean material in the sense that the background carbon and oxygen nuclei are spinless (except for 1% abundance ^{13}C and 0.3% ^{17}O), but f is relatively small. Paramagnetic centres are introduced by dissolving a suitable compound. Ammonia has a larger dilution factor, but has the drawback that the spin-1 ^{14}N nuclei introduce a polarized background which must be corrected for. Solid ammonia must be irradiated at $\sim$ 80 K, e.g., with MeV electrons to introduce the paramagnetic radicals. The use of $^{15}NH_3$ with spin-$\frac{1}{2}$ ^{15}N nuclei was not feasible in our experiment because of the high cost. Deuterated ammonia has a higher dilution factor than that of deuterated butanol, but requires a secondary irradiation at 4 K inside our equipment in order to obtain high polarization [22]. This was not possible in our experimental situation.

To compare the two proton target materials we consider the statistical errors of the spin asymmetries, which are inversely proportional to $\sqrt{x_m \rho} f P$, assuming that the target volume and beam flux are the same. Here x_m is the packing fraction, ρ is the density and P is the average target nuclear polarization. Using the values of the parameters given in Table 2, it is found that the statistical error for the ammonia target is reduced by a factor of 0.83 in comparison to a butanol target. This gain in accuracy is the result of the larger value of the dilution factor, in spite of the lower packing fraction and the lower density of ammonia.

The low packing fraction was due to the irregular shape of the ammonia chips and the low density of ammonia which made it difficult to fill the long target cells, as the chips tended to float on the liquid nitrogen during loading (see Sec. 3.2).

Table 2: Typical parameter values for butanol and ammonia target materials.

	Packing fraction x_m	Density ρ at 77 K (g/cm^3)	Dilution factor $< f >$	Polarization P_{av} (Year)
Butanol	0.62 ± 0.04	0.985	0.12	0.86 (1993)
Ammonia	0.58 ± 0.01	0.853	0.15	0.89 (1996)

3.1.1 Preparation of Normal and Deuterated Butanol

The butanol material was doped by dissolving in it the paramagnetic complex EHBA-Cr(V) [23]. The mass composition by weight of the target material was 78.5% 1-butanol, 12% 2-butanol, 5% water, and 4.5% EHBA-Cr(V) for the normal butanol material. For the deuterated butanol material 91.4% 1-butanol, 4.6% water, and 4% EHBA-Cr(V) was used, for which the components were taken in their perdeuterated form. The deuteration level of this target material was 99.4%. Water was added to promote glass formation, necessary to obtain a homogeneous distribution of the dopant. Together with a uniform cooling of the material, this was crucial for a homogeneous distribution of the polarization. The liquid mixture of the deuterated butanol and its additives was solidified into spherical beads of 1.8 mm diameter by dropping the liquid solution through a needle onto the surface of a liquid nitrogen bath. The droplets of 3 μl volume froze within 4 to 5 seconds and then sank to the bottom of the bath. An apparatus [24] was built to obtain a fast production of the needed quantity of around half a million beads. For that purpose the liquid nitrogen bath was constructed with separate compartments, which moved in succession under two dripping needles. A similar procedure was used for the normal butanol material resulting in beads of 1 to 3 mm diameter. Detailed studies of the butanol target materials were carried out [24]. The low-temperature densities of butanol and deuterated butanol materials were measured to be 0.985 ± 0.031 g/cm^3 and 1.106 ± 0.012 g/cm^3, respectively.

3.1.2 Preparation of Ammonia

For the 3 litres of solid ammonia which had to be prepared for this experiment, a new solidification apparatus with a continuous cooling system was built. The solidification proceeded as follows. Ammonia gas was first condensed in a glass tube at 240 K using an ethanol bath cooled by cold nitrogen gas. When the ammonia gas flow was switched off after about 150 cm^3 of ammonia was liquified, the material immediately started to freeze at the tube wall. Filling the glass cylinder with 500 mbar of argon allowed the liquid to freeze very homogeneously to form a transparent block of ammonia ice. It was then crushed into pieces under liquid nitrogen and sifted to 2 to 3 mm chip size.

To create $\dot{N}H_2$ radicals [25] by irradiation at a low temperature, the sample was immersed in a liquid argon bath at 87 K using a cryostat of which an initial version is described in Ref. [26], but with some modifications in order to guarantee constant conditions for the irradiation of the whole amount of the target material [27].

The irradiation was performed at the Bonn University with 20 MeV electrons and a beam current of 30 μA. The charge collected by the sample container was used as a relative measure for the density of the implanted paramagnetic centres. The constraint of dose homogeneity limited the batch size to 150 cm^3. The geometry of the container and the rotation of the sample produced a sufficiently homogeneous irradiation of the material. This could be judged from the uniform blue colour of the material after the irradiation as well as from the similar polarization behaviour of different small samples which were tested. The density of paramagnetic centres was estimated to be $6 \cdot 10^{19}$ cm^{-3} from previous measurements [25].

retuned to the lower Larmor frequency for protons in a 0.5 T field. This coil was solely used for monitoring purposes; a TE calibration was not available.

The proton relaxation time at 0.5 T and at about 50 mK was long enough to interpolate the polarization decay using a linear function which was valid to a high accuracy. The loss of polarization was only about 1% in 12 hours. During the $A_\perp^p$ data taking period of 17 days with 100 GeV muons [3] the polarization was reversed 10 times, resulting in an average polarization $|P|_{av} = 80\%$.

For the deuterated target the relaxation times were shorter and in order to use the beam time most effectively the field was ramped to 0.5 T while the dilution refrigerator was still cooling down. Assuming an exponential temperature dependence of the relaxation time the polarization decay was calculated using the temperature data (see Fig. 21). The additional error due to this procedure was at most 0.5%. During the $A_\perp^d$ data taking period of 14 days with 190 GeV muons [6] the polarization was reversed five times, and the average polarization was $|P|_{av} = 42\%$.

6 Summary and Concluding Remarks

The performance of a polarized target should not be solely characterized by the maximum polarization obtained but rather by the average polarization during the data taking of the DIS experiment. To cancel false asymmetries the spin directions in our double cell target were reversed fairly often by rotating the magnetic field in an automated fashion. Further cancellation of false asymmetries was done by polarization reversals by DNP every 2 to 3 weeks. Therefore, a rapid polarization build-up was essential in order to avoid loss of beam time. This was also important to recover the polarization quickly after incidents such as power failures. Considerable effort was invested to increase the reliability and user-friendliness of the target operation. We have achieved high degrees of polarization in all of our experiments.

Typical polarization built-up curves for the butanol, d-butanol and ammonia targets are shown in Fig. 22. In all cases FM has been used. In the case of the proton target, about 95% of the maximum polarization was obtained after 10 hours of DNP and the maximum was reached in 24 hours. In contrast, the build-up of the deuteron polarization was much slower, as about 40 hours were needed to reach 95% of the maximum values. After the initial nearly exponential growth, a very slow, almost linear, trend was seen and the maximum polarization was reached after 180 hours of DNP. The microwave power was decreased in the course of DNP to lower the lattice temperature. For the ammonia target somewhat higher microwave power was needed and correspondingly the temperatures were higher.

The maximum polarizations reached with different materials are listed in Table 15. The average degrees of polarization $|P_{av}|$ and their total errors are also given. The considerably larger polarization time constant of ammonia is probably due to the lower density of paramagnetic centres. The average polarization depends also on external factors such as the number of polarization reversals and cannot be directly used to compare the materials. As an example, $|P^+ - P^-|_{av}$ during the 1995 data taking is shown in Fig. 11.

The lower polarization of the deuteron target is compensated by the higher dilution factor. The nuclear spin temperatures corresponding to these polarization values are about 1 mK for the deuterated target materials. The fact that the negative polarization is higher can be qualitatively understood in the framework of the spin temperature theory [79], by the observation that the shape of the EPR absorption line is steeper on the high-frequency side.

Our polarized target with a thickness of $6.8 \cdot 10^{24}$ polarized nucleons per cm^2 is the largest ever used. It was the only means to reach satisfactory statistical accuracy with the limited intensity of the muon beam.

For the NMR measurements we have analyzed the Q-meter circuit very carefully and

Table 15: Average polarizations $P_{av} = |P^+ - P^-|/2$ and their total errors for the different target materials, together with the built-up time $\tau_{0.7}$ to reach 70% of the maximum polarizations P^+_{max} and P^-_{max}.

Material	P_{av} (%)	$\Delta P_{av}/P_{av}$ (%)	$\tau_{0.7}$ (h)	P^+_{max} (%)	P^-_{max} (%)
Butanol	86	3.2	1.5	+94	-94
D-butanol	51	2.0	2.5	+51	-60
Ammonia	89	2.7	3.5	+89	-91

gained understanding of the nonlinearities and the corrections involved. An effort was made to accurately measure the proton and deuteron polarizations with several coils in each cell. Although the NMR coils did not sample the complete cell volumes, we showed that the additional error by this incomplete sampling was small, and that we determined in all SMC measurements the target polarizations with a 3% relative error or better.

The frequency modulation (FM) effect, discovered in 1992 in the refurbished EMC target, increased the deuteron polarization by a factor of 1.7 and allowed us to reach a record deuteron polarization of $-60\,\%$ at 2.5 T.

We have measured the ^{14}N polarization carefully, confirming that the EST hypothesis was closely valid in the ammonia material in a 2.5 T field. The corrections to the measured deep inelastic scattering asymmetries were estimated more precisely than in earlier work [80, 81].

In the future, a similar target design will be employed by the COMPASS collaboration [82] to search for the gluon contribution to the nucleon spin. The superconducting magnet will be replaced by a new one with a much larger opening angle to track particles with high transverse momenta. In addition, the target diameter will be smaller by a factor of 2 owing to a better focusing of the muon beam. ^{6}LiD might be introduced as the deuteron material because of its larger fraction of polarizable nucleons compared to deuterated alcohols or ammonia.

References

[1] SMC, B. Adeva et al., Phys. Lett. B **302** (1993) 533.
[2] SMC, D. Adams et al., Phys. Lett. B **329** (1994) 399; Erratum, Phys. Lett. B **339** (1994) 332.
[3] SMC, D. Adams et al., Phys. Lett. B **336** (1994) 125.
[4] SMC, D. Adams et al., Phys. Lett. B **357** (1995) 248.
[5] SMC, B. Adeva et al., Phys. Lett. B **369** (1996) 93.
[6] SMC, D. Adams et al., Phys. Lett. B **396** (1997) 338.
[7] SMC, B. Adeva et al., Phys. Rev. D **56** (1997) 5330.
[8] SMC, B. Adeva et al., Phys. Lett. B **412** (1997) 414.
[9] SLAC E142, P. L. Anthony et al., Phys. Rev. Lett. **71** (1993) 959.
[10] SLAC E142, P. L. Anthony et al., Phys. Rev. D **54** (1996) 6620.
[11] SLAC E143, K. Abe et al., Phys. Rev. Lett. **74** (1995) 346.
[12] SLAC E143, K. Abe et al., Phys. Rev. Lett. **75** (1995) 25.
[13] SLAC E143, K. Abe et al., Phys. Lett. B **364** (1995) 61.
[14] SLAC E143, K. Abe et al., Phys. Rev. Lett. **76** (1996) 587.
[15] SLAC E154, K. Abe et al., Phys. Rev. Lett. **79** (1997) 26.
[16] SLAC E154, K. Abe et al., Phys. Lett. **404** (1997) 377.
[17] HERMES, K. Ackerstaff et al., Phys. Lett. **404** (1997) 383.
[18] S. C. Brown et al., *Proc. 4th Int. Workshop on Polarized Target Materials and Techniques*, Bad Honnef (Germany), W. Meyer, ed. (3-6 Sept. 1984) 102.

[19] SMC, B. Adeva et al., Nucl. Instr. Meth. A **349** (1994) 334.
[20] J. Kyynäräinen, Nucl. Instr. Meth. A **356** (1995) 47.
[21] A. Abragam and M. Goldman, Rep. Prog. Phys. **41** (1978) 395.
[22] W. Meyer et al., Nucl. Instr. and Meth. **227** (1984) 35.
[23] M. Krumpolc and J. Roček, J. Am. Chem. Soc., **101** (1979) 3206; M. Krumpolc, D. Hill and H.B. Stuhrmann, *Proc. 9th Int. Symposium on High Energy Spin Physics*, Bonn 1990, W. Meyer, E. Steffens and W. Thiel, eds., Vol. 2 (Springer, Berlin, 1991) 340.
[24] S. Bültmann et al., Nucl. Instr. Meth. A **356** (1995) 102.
[25] W. Meyer et al., Nucl. Instr. and Meth. **215** (1983) 65.
[26] S. Brown et al., *Proc. 4th Int. Workshop on Polarized Target Materials and Techniques*, Bad Honnef (Germany), W. Meyer, ed. (3-6 Sept. 1984) 66.
[27] SMC, B. Adeva et al., Nucl. Inst. Meth. A **419** (1998) 60.
[28] O.V. Lounasmaa, *Experimental Principles and Methods Below 1K*, (Academic Press, London, 1974) 265.
[29] T.O. Niinikoski, Nucl. Instr. and Meth. **192** (1982) 151; T.O. Niinikoski and J.-M. Rieubland, *Proc. Nineth Int. Cryogenic Eng. Conf. (ICEC9)*, K. Yasukochi and H. Nagano eds, Butterworth, Guilford, UK (1982) 580.
[30] T.O. Niinikoski, *Proc. Sixth Int. Cryogenic Eng. Conf. (ICEC6)*, K. Mendelssohn ed., Grenoble (France), 11-14 May (1976) 102.
[31] J.-M. Le Goff et al., Nucl. Instr. Meth. A **356** (1995) 96.
[32] A. Daël et al., IEEE Trans. on Magnetics **28** (1992) 560.
[33] R. H. Dicke, Phys. Rev. **93** (1954) 99; Yu. F. Kisselev et al., Zh. Eksp. Teor. Fiz. **94** (2) (1988) 344 [Sov. Phys. JETP **67** (1988) 413].
[34] J. F. M. van Gelder, M.Sc. Thesis, Delft Univ. of Technology, June 1991; S. Ishimoto et al., *Proc. 9th Int. Symposium on High Energy Spin Physics*, Bonn 1990, W. Meyer, E. Steffens and W. Thiel, eds., Vol. 2 (Springer, Berlin, 1991) 369.
[35] G. R. Court, D. W. Gifford, P. Harrison, W. G. Heyes, and M. A. Houlden, Nucl. Inst. Meth. A **324** (1993) 433.
[36] T. O. Niinikoski and A. Rijllart, Nucl. Inst. Meth. A **199** (1982) 485.
[37] N. Hayashi et al., Nucl. Inst. Meth. A **356** (1995) 91.
[38] S. D. Dhawan, IEEE Trans. Nucl. Sci. **NS-39** (1992) 1331.
[39] S. D. Dhawan et al., IEEE Trans. Nucl. Sci. **NS-43** (1996) 2128.
[40] M. Goldman, J. Magn. Res. **17** (1975) 393.
[41] T.O. Niinikoski, Proc. of the 2^{nd} Workshop on Polarized Target Materials, G.R. Court, S.F.J. Cox, D.A. Cragg and T.O. Niinikoski (eds.), Report RL-80-080, SRC, Rutherford Laboratory (1980) 80.
[42] Yu. F. Kisselev, C. M. Dulya, and T. O. Niinikoski, Nucl. Instr. Meth. A **354** (1995) 249.
[43] J.D. Jackson, *Classical Electrodynamics*, 2nd ed. (John Wiley & Sons, New York, 1975) 311.
[44] G. Arfken, *Mathematical Methods for Physicists*, 3rd ed. (Academic Press, New York, 1985) 425.
[45] C. M. Dulya, Ph. D. Thesis, University of California, Los Angeles (1996).
[46] C. M. Dulya, Nucl. Instr. Meth. A **356** (1995) 88.
[47] Y. K. Semertzidis, Nucl. Instr. Meth. A **356** (1995) 83.
[48] C. M. Dulya et al., Nucl. Instr. Meth. A **398** (1997) 109.
[49] O. Hamada et al., Nucl. Instr. and Meth., **189** (1981) 561.
[50] G. D. Wait et al., Nucl. Instr. and Meth., **A274** (1989) 515.
[51] F. Sperisen, Nucl. Instr. Meth. A **260** (1987) 455.
[52] A. Abragam, *Principles of Nuclear Magnetism* (Clarendon Press, Oxford, 1961).

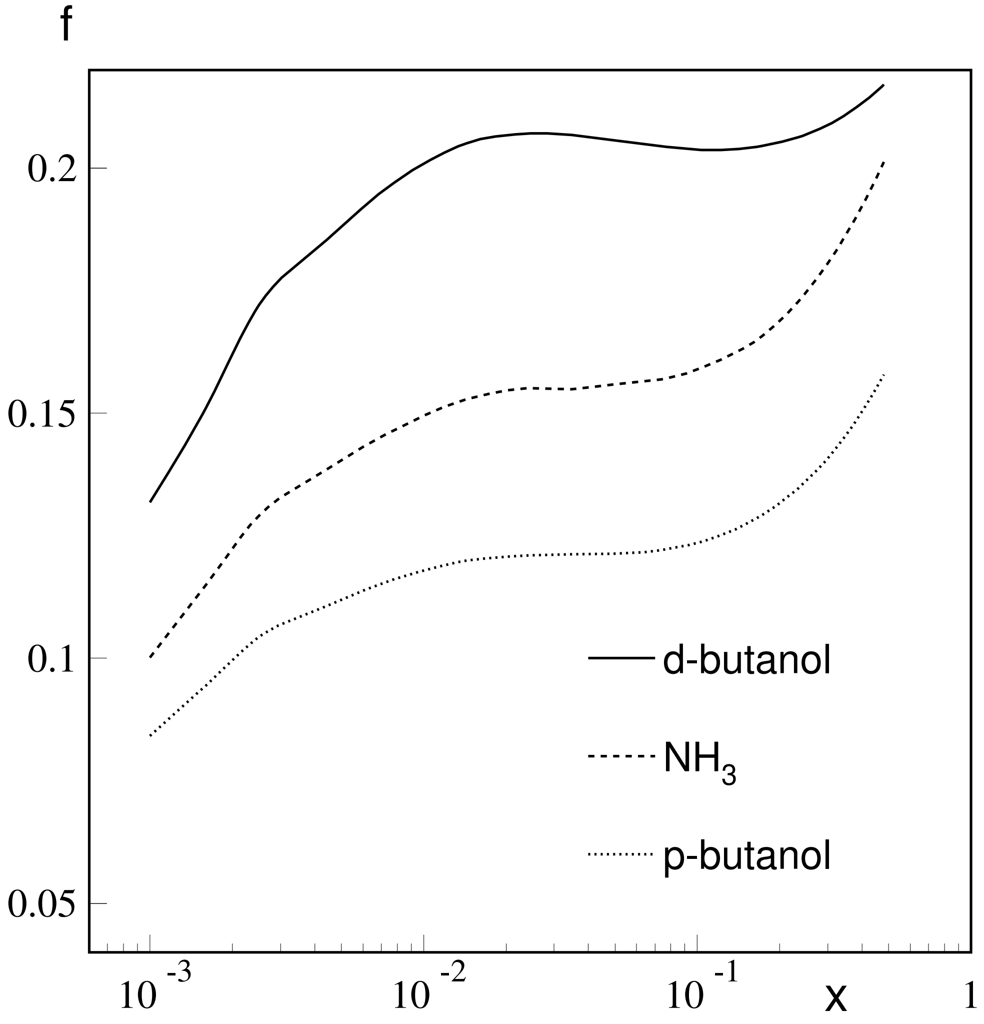

Figure 2: The dilution factors f for the different target materials as function of Bjorken x. The curves (from top to bottom) correspond to deuterated butanol, ammonia and butanol.